Eikonal perturbation theory in photoionization

F. Cajiao Vélez[1], K. Krajewska[1,2], and J. Z. Kamiński[1]

[1]Institute of Theoretical Physics, Faculty of Physics, University of Warsaw, Pasteura 5, 02-093 Warszawa, Poland
[2] Department of Physics and Astronomy, University of Nebraska, Lincoln, Nebraska 68588-0299, USA

E-mail: katarzyna.krajewska@fuw.edu.pl

Abstract. The eikonal perturbation theory is formulated and applied to photoionization by strong laser pulses. A special emphasis is put on the first order approximation with respect to the binding potential, which is known as the *generalized eikonal approximation* [2015 *Phys. Rev. A* **91** 053417]. The ordinary eikonal approximation and its domain of applicability is derived from the generalized eikonal approximation. While the former approach is singular for the electron trajectories which return to the potential center, the generalized eikonal avoids this problem. This property makes it a promising tool for further investigations of rescattering and high-order harmonic generation processes.

1. Introduction

The strong-field approximation (SFA), originated from works of Keldysh [1], Faisal [2] and Reiss [3], has had a pivotal role in the development of strong-laser physics. It describes the situation when the laser field is considered to be much more intense than the atomic interaction experienced by ionized electrons with their residual ions. In other words, it neglects the interaction of electrons with their parent ions after ionization. While frequently used, its application to the analysis of photoionization of neutral atoms remains questionable due to the long-range nature of the Coulomb potential. Thus, many efforts have been undertaken in order to include the effects of long-range potentials into this theory. For example, in the improved strong-field approximation, the Coulomb interaction is included as a perturbation, leading to the Born series expansion [4, 5, 6]. In this context, the Coulomb-Volkov ansatz [7, 8, 9, 10], which accounts for the asymptotic phase of the atomic field-free wave function, was also introduced. The latter, combined with the quantum trajectory method [11, 12, 13, 14, 15], have made considerable improvements in the SFA to include the Coulomb interactions [14].

In another effort to introduce the binding potential in the theory, the eikonal approximation was applied to describe photoionization processes. In general, this quasiclassical approximation is extensively used to analyze scattering processes at high energies and small angles [16, 17], regime for which the perturbation theory is not good enough (see, also Ref. [18]). It has been applied, for instance, to study the electron scattering with laser fields in the relativistic and non-relativistic frameworks [19]. The application of the so-called Molière-Glauber eikonal [20, 21] to ionization provided a new tool to treat photoelectron dynamics in the presence of strong laser fields [22, 23]. In this context, the eikonal-Volkov approximation was also introduced [24, 25]. This consisted in including the laser field in full extent by means of the Volkov wave function,

together with the ionic potential treated within the eikonal approximation. This approach was further developed to describe molecular ionization [26].

Following our recent work [27], we present the eikonal perturbation theory and its application to strong-field ionization. This approach in the first order with respect to the binding potential, which we call the generalized eikonal approximation, avoids a singularity at the potential center. Thus, in contrast to the original eikonal approximation [20, 21], it is not singular for returning electron trajectories. This is illustrated in this paper numerically by direct comparison between the generalized and ordinary eikonals calculated along the complex-time quantum trajectories. As a result, we avoid an unphysical behavior of probability distributions of ionization, which is observed when the ordinary eikonal approximation is used [27].

Throughout this paper, the atomic units (a.u.) are used, in which $\hbar = 1$ but we explicitly keep the electron charge ($e < 0$) and mass (m) in the equations. In numerical calculations, both quantities are set to $|e| = 1$ and $m = 1$.

2. Generalized eikonal approximation

Consider an electron of charge $e < 0$ and mass m placed in an external potential $V(\boldsymbol{r}, t)$ and in a laser field; the latter being characterized by the vector potential $\boldsymbol{A}(t)$. The propagator that describes the electron dynamics in the velocity gauge, $K_V(\boldsymbol{r}, t; \boldsymbol{r}', t')$, satisfies the equation,

$$\Big(-\mathrm{i}\frac{\partial}{\partial t'} - \frac{1}{2m}[\mathrm{i}\boldsymbol{\nabla}' - e\boldsymbol{A}(t')]^2 - V(\boldsymbol{r}', t')\Big)K_V(\boldsymbol{r}, t; \boldsymbol{r}', t') = \mathrm{i}\delta(t - t')\delta(\boldsymbol{r} - \boldsymbol{r}'). \tag{1}$$

We seek for the solution of this equation using the proper time representation [19],

$$K_V(\boldsymbol{r}, t; \boldsymbol{r}', t') = \int_0^\infty \mathrm{d}s \int \frac{\mathrm{d}\Omega\, \mathrm{d}^3k}{(2\pi)^4} \exp\Big[-\mathrm{i}\Omega(t - t') + \mathrm{i}\boldsymbol{k}\cdot(\boldsymbol{r} - \boldsymbol{r}') + \mathrm{i}s\big(\Omega - \frac{\boldsymbol{k}^2}{2m} + \mathrm{i}\varepsilon\big) + \mathrm{i}\Phi_{\boldsymbol{k}}(t', s) + \mathrm{i}\chi_{\boldsymbol{k}}(\boldsymbol{r}', t', s)\Big], \tag{2}$$

where $\varepsilon > 0$ is introduced for convergence. Plugging this ansatz into Eq. (1), we obtain two independent equations satisfied by the unknown functions, $\Phi_{\boldsymbol{k}}(t', s)$ and $\chi_{\boldsymbol{k}}(\boldsymbol{r}', t', s)$,

$$\Big(\frac{\partial}{\partial t'} - \frac{\partial}{\partial s}\Big)\Phi_{\boldsymbol{k}}(t', s) = -\frac{e}{m}\boldsymbol{A}(t')\cdot\big[\boldsymbol{k} - \frac{e}{2}\boldsymbol{A}(t')\big], \tag{3}$$

$$\Big(\frac{\partial}{\partial t'} - \frac{\partial}{\partial s}\Big)\chi_{\boldsymbol{k}}(\boldsymbol{r}', t', s) = -\frac{1}{m}\big[\boldsymbol{k} - e\boldsymbol{A}(t')\big]\cdot\boldsymbol{\nabla}'\chi_{\boldsymbol{k}}(\boldsymbol{r}', t', s) + V(\boldsymbol{r}', t') + \frac{1}{2m}\big(\boldsymbol{\nabla}'\chi_{\boldsymbol{k}}(\boldsymbol{r}', t', s)\big)^2 - \frac{\mathrm{i}}{2m}\Delta'\chi_{\boldsymbol{k}}(\boldsymbol{r}', t', s). \tag{4}$$

Eq. (3) can be easily solved, leading to

$$\Phi_{\boldsymbol{k}}(t', s) = \int_{t'}^{t'+s} \mathrm{d}\tau\, \frac{e}{m}\boldsymbol{A}(\tau)\cdot\big[\boldsymbol{k} - \frac{e}{2}\boldsymbol{A}(\tau)\big]. \tag{5}$$

Eq. (4), on the other hand, is a nonlinear second order differential equation which can be solved explicitly only for particular potentials. Other than that, one can formulate a general approach of treating Eq. (4) perturbatively.

As shown in Ref. [27], the solution of Eq. (4), the so-called *eikonal*, can be represented in the form

$$\chi_{\boldsymbol{k}}(\boldsymbol{r}', t', s) = -\int_{t'}^{t'+s} \mathrm{d}\sigma \int \mathrm{d}^3\rho \left(\frac{m}{2\pi\mathrm{i}(\sigma - t')}\right)^{3/2} \exp\Big(\frac{\mathrm{i}m}{2(\sigma - t')}[\boldsymbol{R}_{\boldsymbol{k}}(\boldsymbol{r}', t', \sigma) - \boldsymbol{\rho}]^2\Big) \times W_{\boldsymbol{k}}(\boldsymbol{\rho}, \sigma, t' + s - \sigma). \tag{6}$$

Here,

$$\boldsymbol{R}_{\boldsymbol{k}}(\boldsymbol{r}',t',\sigma)=\boldsymbol{r}'+\frac{1}{m}\int_{t'}^{\sigma}\mathrm{d}\tau[\boldsymbol{k}-e\boldsymbol{A}(\tau)] \tag{7}$$

is interpreted as a free electron trajectory in the laser field and $W_{\boldsymbol{k}}(\boldsymbol{r}',t',s)$ is defined as

$$W_{\boldsymbol{k}}(\boldsymbol{r}',t',s)=V(\boldsymbol{r}',t')+\frac{1}{2m}\big(\boldsymbol{\nabla}'\chi_{\boldsymbol{k}}(\boldsymbol{r}',t',s)\big)^2. \tag{8}$$

This is the starting point for developing the eikonal perturbation theory. Specifically, in the first approximation, when

$$W^{(1)}_{\boldsymbol{k}}(\boldsymbol{r}',t',s)\approx V(\boldsymbol{r}',t'), \tag{9}$$

one obtains

$$\chi^{(1)}_{\boldsymbol{k}}(\boldsymbol{r}',t',s)=-\int_{t'}^{t'+s}\mathrm{d}\sigma\int\mathrm{d}^3\rho\left(\frac{m}{2\pi\mathrm{i}(\sigma-t')}\right)^{3/2}\exp\Big(\frac{\mathrm{i}m}{2(\sigma-t')}[\boldsymbol{R}_{\boldsymbol{k}}(\boldsymbol{r}',t',\sigma)-\boldsymbol{\rho}]^2\Big)V(\boldsymbol{\rho},\sigma). \tag{10}$$

In the following, we shall call $\chi^{(1)}_{\boldsymbol{k}}(\boldsymbol{r}',t',s)$ the *generalized eikonal*. Note that it also defines the propagator (2) in the first order eikonal approximation,

$$K^{(1)}_V(\boldsymbol{r},t;\boldsymbol{r}',t')=\int\frac{\mathrm{d}^3k}{(2\pi)^3}\exp\Big[\mathrm{i}\boldsymbol{k}\cdot(\boldsymbol{r}-\boldsymbol{r}')-\mathrm{i}(t-t')\frac{\boldsymbol{k}^2}{2m}+\mathrm{i}\Phi_{\boldsymbol{k}}(t',t-t')+\mathrm{i}\chi^{(1)}_{\boldsymbol{k}}(\boldsymbol{r}',t',t-t')\Big], \tag{11}$$

where, in Eq. (2), we have explicitly performed the integrals over s and Ω.

For our further purpose, let us represent the generalized eikonal (10) such that

$$\chi^{(1)}_{\boldsymbol{k}}(\boldsymbol{r}',t',s)=-\int_{t'}^{t'+s}\mathrm{d}\sigma\,V^{(1)}_{\mathrm{eff}}\big(\boldsymbol{R}_{\boldsymbol{k}}(\boldsymbol{r}',t',\sigma),t',\sigma\big), \tag{12}$$

where we have introduced the effective potential,

$$V^{(1)}_{\mathrm{eff}}\big(\boldsymbol{R}_{\boldsymbol{k}}(\boldsymbol{r}',t',\sigma),t',\sigma\big)=\int\mathrm{d}^3\rho\left(\frac{m}{2\pi\mathrm{i}(\sigma-t')}\right)^{3/2}\exp\Big(\frac{\mathrm{i}m}{2(\sigma-t')}[\boldsymbol{R}_{\boldsymbol{k}}(\boldsymbol{r}',t',\sigma)-\boldsymbol{\rho}]^2\Big)V(\boldsymbol{\rho},\sigma). \tag{13}$$

As argued in Ref. [27], the effective potential differs from the classical one, $V(\boldsymbol{r},t)$, by quantum corrections which vanish in the limit $\hbar\to 0$. This means that the effective potential accounts for the spreading of the electron wave packet during the time evolution. Thus, it eliminates the problem with rescattering trajectories, as it will be illustrated numerically in Sec. 4.

In closing this Section we note that, for the generalized eikonal approximation [Eq. (9)] to be applicable, it must hold that $\big(\boldsymbol{\nabla}'\chi_{\boldsymbol{k}}(\boldsymbol{r},t,s)\big)^2\ll 2m|V(\boldsymbol{r},t)|$. This condition is very well satisfied for numerical illustrations presented in Sec. 4. Following the first order approximation, we note that Eq. (8) allows us to define the recurrence relation,

$$W^{(n+1)}_{\boldsymbol{k}}(\boldsymbol{r}',t',s)=V(\boldsymbol{r}',t')+\frac{1}{2m}\big(\boldsymbol{\nabla}'\chi^{(n)}_{\boldsymbol{k}}(\boldsymbol{r}',t',s)\big)^2 \tag{14}$$

and, as a consequence, to define the generalized eikonal (6) in subsequent orders. Investigations of higher order terms in the eikonal perturbation theory are, however, beyond the scope of this paper.

3. Generalized eikonal for the Coulomb potential

For the Coulomb potential describing the interaction of an electron and a nucleus of charge $-Ze$, where $Z = 1, 2, ...$ is the atomic number, we have $V(\boldsymbol{r}, t) = -Z\alpha c/r$. Here, $\alpha = e^2/(4\pi\varepsilon_0 c)$ is the fine structure constant (in a.u., $\alpha c = 1$). Thus, the generalized eikonal defined in (10) becomes

$$\chi^{(1)}_{\boldsymbol{k}}(\boldsymbol{r}', t', s) = \int_{t'}^{t'+s} \mathrm{d}\sigma \int \mathrm{d}^3\rho \left(\frac{m}{2\pi \mathrm{i}(\sigma - t')}\right)^{3/2} \frac{Z\alpha c}{\rho} \exp\Big(\frac{\mathrm{i}m}{2(\sigma - t')}[\boldsymbol{R}_{\boldsymbol{k}}(\boldsymbol{r}', t', \sigma) - \boldsymbol{\rho}]^2\Big). \quad (15)$$

Performing the integral over $\boldsymbol{\rho}$, we arrive at

$$\chi^{(1)}_{\boldsymbol{k}}(\boldsymbol{r}', t', s) = Z\alpha c \int_{t'}^{t'+s} \mathrm{d}\sigma \, \frac{1}{|\boldsymbol{R}_{\boldsymbol{k}}(\boldsymbol{r}', t', \sigma)|} \mathrm{erf}\Big(\sqrt{\frac{m}{2\mathrm{i}(\sigma - t')}}\, |\boldsymbol{R}_{\boldsymbol{k}}(\boldsymbol{r}', t', \sigma)|\Big), \quad (16)$$

where $\mathrm{erf}(z)$ is the error function.

The originally used eikonal [20, 21, 19, 26],

$$\chi_{\boldsymbol{k},\mathrm{original}}(\boldsymbol{r}', t', s) = Z\alpha c \int_{t'}^{t'+s} \mathrm{d}\sigma \, \frac{1}{|\boldsymbol{R}_{\boldsymbol{k}}(\boldsymbol{r}', t', \sigma)|}, \quad (17)$$

is recovered from Eq. (16), if $\sqrt{\frac{m}{2(\sigma - t')}}\, |\boldsymbol{R}_{\boldsymbol{k}}(\boldsymbol{r}', t', \sigma)| \gg 1$. Note that this condition is satisfied for short-time intervals $\sigma \approx t'$, given that $|\boldsymbol{R}_{\boldsymbol{k}}(\boldsymbol{r}', t', \sigma)| \neq 0$. For $\sigma \not\approx t'$, it requires that $|\boldsymbol{R}_{\boldsymbol{k}}(\boldsymbol{r}', t', \sigma)| \not\to 0$. As it was shown in Ref. [27], in the limit when $|\boldsymbol{R}_{\boldsymbol{k}}(\boldsymbol{r}', t', \sigma)| \to 0$, the generalized eikonal (16) presents an integrable singularity. This suggests that the generalized eikonal approximation is applicable even to cases when the electron trajectory can return back to the origin of the Coulomb potential. This is in contrast to the original eikonal (17), which diverges logarithmically for such trajectories.

4. Application of the generalized eikonal approximation to ionization

In this paper, we apply the generalized eikonal approximation to ionization of a hydrogen-like atom by a modulated laser pulse. We assume that the pulse lasts for time T, i.e., it is described by the electric field $\boldsymbol{\mathcal{E}}(t)$ which vanishes for $t < 0$ and $t > T$. The pulse duration T defines the fundamental frequency of field oscillations, $\omega = 2\pi/T$. One can also introduce the field phase, $\phi = \omega t$, which allows us to rewrite the above condition such that $\boldsymbol{\mathcal{E}}(\phi)$ vanishes for $\phi < 0$ and $\phi > 2\pi$. We also assume that the driving pulse is linearly polarized along the z-axis.

4.1. Model of the laser pulse

In the dipole approximation, we describe the laser field by the electric field vector

$$\boldsymbol{\mathcal{E}}(\phi) = \mathcal{E}_0 f_{\mathcal{E}}(\phi) \boldsymbol{e}_z, \quad (18)$$

where $\mathcal{E}_0$ is related to the amplitude of field oscillations. We consider the shape function $f_{\mathcal{E}}(\phi)$ such that

$$f_{\mathcal{E}}(\phi) = \begin{cases} \sin^2(N_{\mathrm{rep}} \frac{\phi}{2}) \sin(N_{\mathrm{rep}}\phi), & \phi \in [0, 2\pi], \\ 0, & \text{otherwise.} \end{cases} \quad (19)$$

This means that the pulse consists of N_{rep} modulations ($N_{\mathrm{rep}} = 1, 2, 3, ...$), each one being a single-cycle pulse. We also define the shape function for the vector potential $\boldsymbol{A}(\phi)$ such that

$$f_A(\phi) = -\int_0^{\phi} f_{\mathcal{E}}(\varphi) \mathrm{d}\varphi, \quad (20)$$

which leads to

$$\boldsymbol{A}(\phi) = \frac{\mathcal{E}_0}{\omega} f_A(\phi) \boldsymbol{e}_z. \quad (21)$$

Note that, for our choice of the shape function (19), the condition $\boldsymbol{A}(2\pi) = \boldsymbol{A}(0) = \boldsymbol{0}$ holds.

4.2. Probability amplitude of ionization using the generalized eikonal approximation
As derived in Ref. [27], under the generalized eikonal approximation, the probability amplitude to ionize a hydrogen-like atom equals

$$\mathcal{A}^{(1)}(\boldsymbol{p}) = -\,\mathrm{i}\int_0^T \mathrm{d}t'\,\mathrm{e}^{\mathrm{i}\frac{\boldsymbol{p}^2}{2m}T-\mathrm{i}E_0t'}\int \mathrm{d}^3r\int \mathrm{d}^3r'\psi_{\boldsymbol{p}}^{(-)*}(\boldsymbol{r})K_L^{(1)}(\boldsymbol{r},T;\boldsymbol{r}',t')(-e\boldsymbol{\mathcal{E}}(t')\cdot\boldsymbol{r}')\psi_0(\boldsymbol{r}'). \quad (22)$$

Here, we assume that $\psi_0(\boldsymbol{r}) = \lambda\sqrt{\frac{\lambda}{\pi}}\mathrm{e}^{-\lambda r}$ is the ground state of a hydrogen-like atom with energy $E_0 = -\frac{\lambda^2}{2m}$ [$\lambda = (Za_0)^{-1}$, a_0 is the Bohr radius] whereas $\psi_{\boldsymbol{p}}^{(-)}(\boldsymbol{r})$ is the scattering state describing the ionized electron of momentum $\boldsymbol{p}$. Note that the probability amplitude (22) is expressed in the length gauge. Thus, $K_L^{(1)}(\boldsymbol{r},T;\boldsymbol{r}',t')$ represents the electron propagator in the length gauge as well. More specifically,

$$K_L^{(1)}(\boldsymbol{r},t;\boldsymbol{r}',t') = \int\frac{\mathrm{d}^3k}{(2\pi)^3}\exp\Big[\mathrm{i}(\boldsymbol{k}-e\boldsymbol{A}(t))\cdot\boldsymbol{r}-\mathrm{i}(\boldsymbol{k}-e\boldsymbol{A}(t'))\cdot\boldsymbol{r}'-\mathrm{i}(t-t')\frac{\boldsymbol{k}^2}{2m} + \mathrm{i}\Phi_{\boldsymbol{k}}(t',t-t')+\mathrm{i}\chi_{\boldsymbol{k}}^{(1)}(\boldsymbol{r}',t',t-t')\Big], \quad (23)$$

which follows from Eq. (11) after applying the gauge transformation [27].

In order to proceed, it was assumed in Ref. [27] that the final electron state $\psi_{\boldsymbol{p}}^{(-)}(\boldsymbol{r})$ is essentially the plane wave. This made it possible to explicitly perform the integral over $\boldsymbol{r}$ in Eq. (22). The remaining integrals were reformulated such that

$$\mathcal{A}^{(1)}(\boldsymbol{p}) = -\mathrm{i}\frac{\mathrm{e}^{\mathrm{i}(\boldsymbol{p}^2/2m-E_0)T}}{\omega}\int_0^{2\pi}\mathrm{d}\phi\int \mathrm{d}^3r'\mathrm{e}^{-\mathrm{i}(\boldsymbol{p}-e\boldsymbol{A}(\phi))\cdot\boldsymbol{r}'}(-e\boldsymbol{\mathcal{E}}(\phi)\cdot\boldsymbol{r}')\psi_0(\boldsymbol{r}')\mathrm{e}^{\mathrm{i}W[\phi,\boldsymbol{p}|\boldsymbol{r}_{\mathrm{cl}}]}. \quad (24)$$

Here, the functional $W[\phi,\boldsymbol{p}|\boldsymbol{r}_{\mathrm{cl}}]$, which depends on the classical electron trajectory,

$$\boldsymbol{r}_{\mathrm{cl}}(\sigma;\boldsymbol{r}',\phi,\boldsymbol{p}) \equiv \boldsymbol{r}_{\mathrm{cl}}(\sigma) = \boldsymbol{R}_{\boldsymbol{p}}\Big(\boldsymbol{r}',\frac{\phi}{\omega},\frac{\sigma}{\omega}\Big), \quad (25)$$

has been introduced. More specifically,

$$W[\phi,\boldsymbol{p}|\boldsymbol{r}_{\mathrm{cl}}] = S[\phi|\boldsymbol{r}_{\mathrm{cl}}] + m\omega\boldsymbol{r}_{\mathrm{cl}}(\phi)\cdot\boldsymbol{r}'_{\mathrm{cl}}(\phi) - \boldsymbol{p}\cdot\boldsymbol{r}_{\mathrm{cl}}(2\pi), \quad (26)$$

with the action and the effective Lagrangian equal to

$$S[\phi|\boldsymbol{r}_{\mathrm{cl}}] = \frac{1}{\omega}\int_\phi^{2\pi}\mathrm{d}\sigma\mathcal{L}_{\mathrm{eff}}(\boldsymbol{r}_{\mathrm{cl}}(\sigma),\boldsymbol{r}'_{\mathrm{cl}}(\sigma),\sigma), \quad (27)$$

$$\mathcal{L}_{\mathrm{eff}}(\boldsymbol{r}_{\mathrm{cl}}(\sigma),\boldsymbol{r}'_{\mathrm{cl}}(\sigma),\sigma) = \frac{m\omega^2}{2}[\boldsymbol{r}'_{\mathrm{cl}}(\sigma)]^2 + e\boldsymbol{\mathcal{E}}(\sigma)\cdot\boldsymbol{r}_{\mathrm{cl}}(\sigma) - V_{\mathrm{eff}}^{(1)}(\boldsymbol{r}_{\mathrm{cl}}(\sigma),\sigma-\phi) + E_0, \quad (28)$$

respectively. Since the effective potential describing the interaction of the photoelectron and its parent ion oscillates rapidly, in Eq. (24) we apply the saddle-point method. While the details of the derivations are presented in Ref. [27], we remind that, instead of classical trajectories, the complex-time quantum trajectories are used in these derivations.

4.3. Complex-time quantum trajectories
The complex-time quantum trajectory is the solution of the classical Newton equation in the laser field,

$$\boldsymbol{r}''_q(\phi;\boldsymbol{p},\phi_s) = \frac{e}{m\omega^2}\boldsymbol{\mathcal{E}}(\phi), \quad (29)$$

where the '*prime*' means the derivative with respect to ϕ. Here, ϕ_s defines the initial phase for which the following conditions are satisfied,

$$\mathrm{Re}[\boldsymbol{r}_q(\phi_s;\boldsymbol{p},\phi_s)]=\boldsymbol{0},\qquad [m\omega\boldsymbol{r}'_q(\phi_s;\boldsymbol{p},\phi_s)]^2=-\lambda^2. \tag{30}$$

It turns out that the initial phase is the solution of the equation,

$$\frac{\partial}{\partial\phi}G(\boldsymbol{p},\phi)\Big|_{\phi=\phi_s}=0, \tag{31}$$

with

$$G(\boldsymbol{p},\phi)=\frac{1}{\omega}\int_0^{\phi}\mathrm{d}\phi'\Big\{\frac{[\boldsymbol{p}-e\boldsymbol{A}(\phi')]^2}{2m}-E_0\Big\}. \tag{32}$$

The quantum trajectories, satisfying the conditions (30), can be written in the form [27]

$$\boldsymbol{r}_q(\phi;\boldsymbol{p},\phi_s)=\frac{\boldsymbol{p}}{m\omega}[\phi-\mathrm{Re}(\phi_s)]+\frac{e}{m}\boldsymbol{\alpha}(\phi)-\frac{e}{m}\mathrm{Re}[\boldsymbol{\alpha}(\phi_s)], \tag{33}$$

where $\boldsymbol{\alpha}(\phi)=-\frac{1}{\omega}\int_0^{\phi}\boldsymbol{A}(\varphi)\mathrm{d}\varphi$. In addition, the trajectories (33) satisfy the conditions,

$$\mathrm{Im}[\boldsymbol{r}_q(\mathrm{Re}\,\phi;\boldsymbol{p},\phi_s)]=\boldsymbol{0},\qquad \mathrm{Im}[\boldsymbol{r}'_q(\mathrm{Re}\,\phi;\boldsymbol{p},\phi_s)]=\boldsymbol{0}. \tag{34}$$

Since we deal with the Coulomb-free trajectories, if the laser pulse is switched off the electron will carry the momentum $\boldsymbol{p}$. In other words,

$$m\omega\boldsymbol{r}'_q(2\pi;\boldsymbol{p},\phi_s)=\boldsymbol{p}. \tag{35}$$

This agrees with the assumption that the electron final state is approximated by the plane wave solution.

4.4. Probability amplitude of ionization using the saddle-point approach

After applying the saddle-point method along with the complex-time quantum trajectories with respect to Eq. (24), the probability amplitude of ionization of a hydrogen-like atom by a finite laser pulse becomes

$$\mathcal{A}^{(1)}_{\mathrm{saddle}}(\boldsymbol{p})=-2\sqrt{\frac{\lambda}{\pi}}\Big(\frac{\pi\lambda}{m\omega}\Big)^2\mathrm{e}^{\mathrm{i}\Phi_0(\boldsymbol{p})}\sum_s\frac{\mathrm{e}^{\mathrm{i}G(\boldsymbol{p},\phi_s)+\mathrm{i}\chi^{(1)}_q(\boldsymbol{p},\phi_s)}}{G''(\boldsymbol{p},\phi_s)}. \tag{36}$$

The summation is over all solutions of Eq. (31) with $\mathrm{Im}[\phi_s]>0$ (since now on, called the *saddle points*). Let us note, however, that the most important contributions to the sum in (36) come from these saddle points which satisfy the conditions,

$$\mathrm{Im}[G(\boldsymbol{p},\phi_s)]>0,\quad \mathrm{Im}[G''(\boldsymbol{p},\phi_s)]>0, \tag{37}$$

and result in the smallest value of $\mathrm{Im}[G(\boldsymbol{p},\phi_s)]$. Therefore, only those points will be considered in our numerical illustrations presented in the next Section. In Eq. (36), we have also introduced the abbreviation $\Phi_0(\boldsymbol{p})=\big(\frac{\boldsymbol{p}^2}{2m}-E_0\big)T-G(\boldsymbol{p},2\pi)$. Moreover, $\chi^{(1)}_q(\boldsymbol{p},\phi_s)$ present there is the generalized eikonal (16) calculated along the quantum trajectory (33) starting at ϕ_s,

$$\chi^{(1)}_q(\boldsymbol{p},\phi_s)=\frac{Z\alpha c}{\omega}\int_{\phi_s}^{2\pi}\mathrm{d}\sigma\frac{1}{|\boldsymbol{r}_q(\sigma;\boldsymbol{p},\phi_s)|}\mathrm{erf}\Big(\sqrt{\frac{m\omega}{2\mathrm{i}(\sigma-\phi_s)}}|\boldsymbol{r}_q(\sigma;\boldsymbol{p},\phi_s)|\Big). \tag{38}$$

Following Eq. (17), one can also define the original eikonal,

$$\chi_{q,\mathrm{original}}(\boldsymbol{p},\phi_s)=\frac{Z\alpha c}{\omega}\int_{\phi_s}^{2\pi}\mathrm{d}\sigma\frac{1}{|\boldsymbol{r}_q(\sigma;\boldsymbol{p},\phi_s)|}. \tag{39}$$

It defines the respective probability amplitude of ionization, which is essentially the same as Eq. (36) except that $\chi^{(1)}_q(\boldsymbol{p},\phi_s)$ has to be replaced by $\chi_{q,\mathrm{original}}(\boldsymbol{p},\phi_s)$.

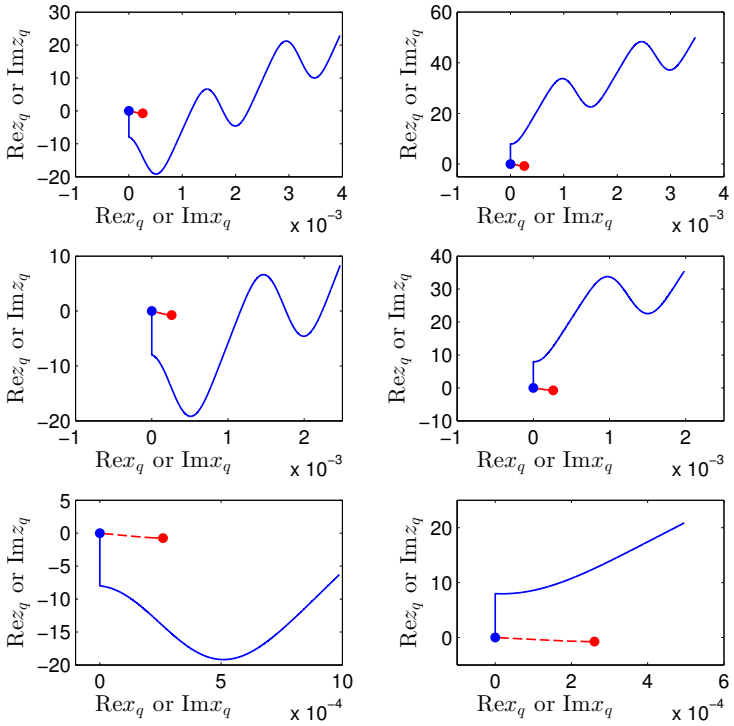

Figure 1. Real (solid blue lines) and imaginary (dashed red lines) parts of the quantum trajectories (in a.u.), calculated from Eq. (33), for an electron with the kinetic energy $E_{\boldsymbol{p}} = 3.13$eV. The electron is ionized by a modulated pulse defined by Eqs. (18) and (19) where $N_{\rm rep} = 3$, $\omega_{\rm L} = 1.55$eV and $I = 3.125 \times 10^{13}$W/cm^2. Each panel represents a trajectory starting at a different saddle point ϕ_s. Only the essential saddle points are considered.

4.5. Numerical illustrations

To illustrate numerically the introduced theory, we calculate first the complex-time quantum trajectories defined by Eq. (33). For this purpose, we consider a Ti:sapphire laser working at frequency $\omega_{\rm L} = 1.55$eV. We assume that it produces a modulated pulse, as defined by Eqs. (18) and (19), which consists of three single-cycle modulations ($N_{\rm rep} = 3$). The averaged intensity carried out by the pulse, which in general is defined as $I = \langle c\varepsilon_0 \boldsymbol{\mathcal{E}}^2 \rangle = \frac{1}{2\pi} \int_0^{2\pi} c\varepsilon_0 \boldsymbol{\mathcal{E}}^2(\phi) \mathrm{d}\phi$, equals $I = 3.125 \times 10^{13}$W/cm^2. Let us also remind that the pulse is linearly polarized in the z-direction. As introduced in Ref. [27], one can define the ponderomotive energy of electron free oscillations in such a laser field, U_p. For the current parameters, $U_p = 1.024\omega_{\rm L}$.

In Fig. 1, we present the quantum trajectories starting at saddle points ϕ_s for a photoelectron that is detected with energy $E_{\boldsymbol{p}} = 3.13\text{eV} \approx 3U_p$ at the polar angle $\theta_{\boldsymbol{p}} = 0.2\pi$. The same but for the electron with energy $E_{\boldsymbol{p}} = 12.22\text{eV} \approx 12U_p$ is shown in Fig. 2. Since the laser field is linearly polarized the results are independent of the azimuthal angle of the electron, $\varphi_{\boldsymbol{p}}$. Actually, for the laser field consider in this example there are 24 saddle points. However, only those saddle points which satisfy the conditions (37) and posses the smallest Im$[G(\boldsymbol{p}, \phi_s)]$ have been chosen for numerical illustrations. As we have checked this numerically, the remaining saddle points have a marginally small contribution to the probability amplitude of ionization (36). Therefore, we do not consider them for the purpose of these and subsequent figures. Here, we plot the real (solid blue lines) and imaginary (dashed red lines) parts of the quantum trajectories which originate from the essential saddle points. As we have checked this, these saddle points relate

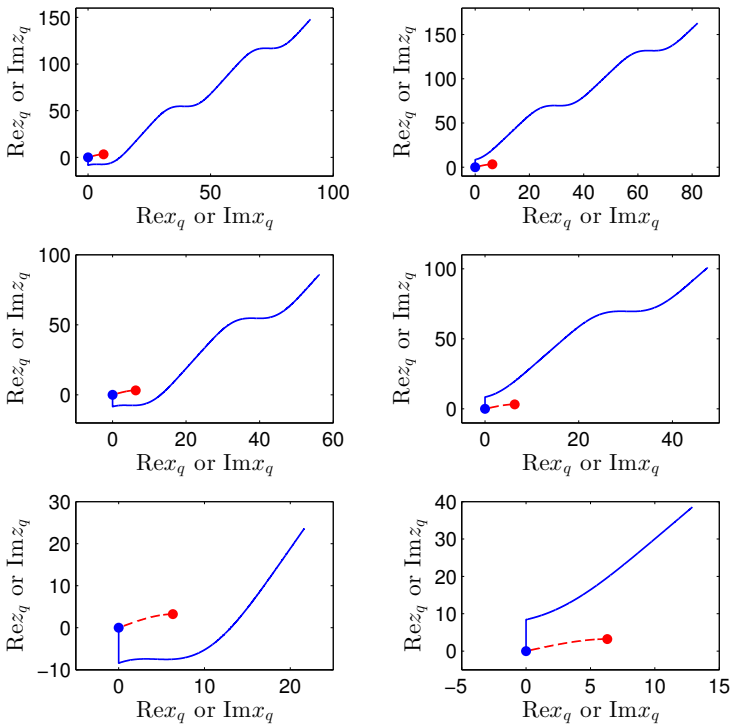

Figure 2. The same as in Fig. 1 but for $E_{\boldsymbol{p}} = 12.22\text{eV}$.

to either the maximum or minimum of the electric field. The trajectories starting at the former points are plotted in the left column of Figs. 1 and 2, whereas the trajectories starting at the latter points are plotted in the right column of Figs. 1 and 2. Note that these trajectories are parametrized by Cartesian coordinates x_q and z_q. When comparing Figs. 1 and 2, we note a significant difference of the scale of x_q.

It can be seen in Fig. 1 that, for $E_{\boldsymbol{p}} = 3.13\text{eV} \approx 3U_p$, the real part of some of the quantum trajectories approach the ion after the electron is ionized. This is shown in the top and middle panels of the left column. For $E_{\boldsymbol{p}} = 12.22\text{eV} \approx 12U_p$ (Fig. 2), already shortly after ionization, x_q acquires large values and the electron never comes back near the potential center. As it will become clear shortly, the trajectories which come back to its center lead to singularities in the formulation based on the original eikonal approximation. Our generalized eikonal approximation avoids this problem.

In Fig. 3, we plot the real and imaginary parts of the original eikonal, $\chi_{q,\,\text{original}}(\boldsymbol{p}, \phi_s)$, which is defined by Eq. (39). The eikonal is calculated along the quantum trajectories which start at the saddle points at either the maximum (solid blue lines) or minimum (dashed red lines) of the laser field. As before, these saddle points fulfill the conditions (37) and have the smallest $\text{Im}[G(\boldsymbol{p}, \phi_s)]$. As we can observe, the real parts of $\chi_{q,\text{original}}(\boldsymbol{p}, \phi_s)$ exhibit the sharp peaks at two instances. This happens for those trajectories which return very close to the origin of the Coulomb potential, and which are plotted in Fig. 1. Note that the fact that the original eikonal is singular for the returning trajectories is a consequence of its definition, i.e., Eq. (39). Moreover, we see in Fig. 3 that the rapid change of $\text{Re}\,\chi_{q,\,\text{original}}(\boldsymbol{p}, \phi_s)$ happens when the photoelectron energy passes through the value $3U_p$. This explains why in Fig. 10 of Ref. [27] the corresponding energy distribution of ionization shows unphysical wiggles around this energy. In contrast, such a behavior is not observed in [27] when the generalized eikonal approximation is used. The reason

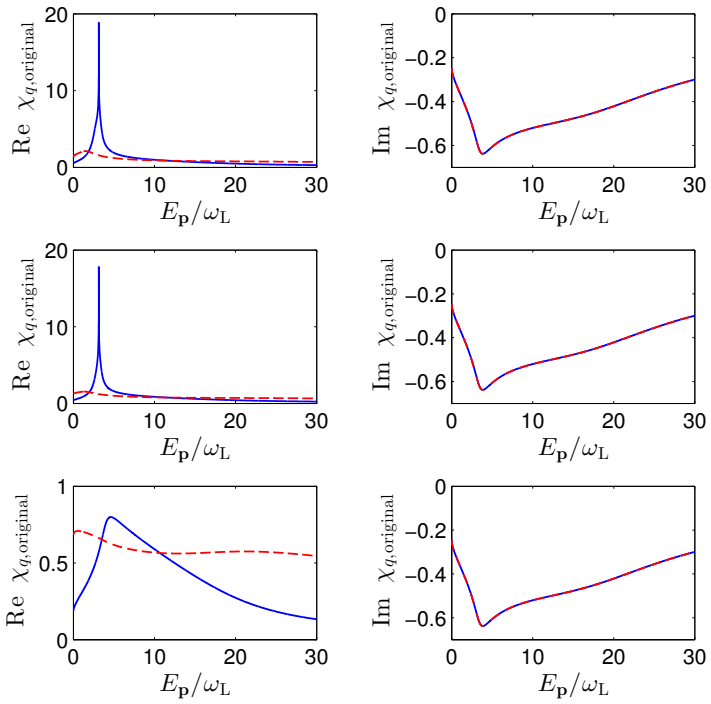

Figure 3. Imaginary and real parts of the original eikonal, $\chi_{q,\,\mathrm{original}}(\boldsymbol{p},\phi_s)$, calculated according to Eq. (39), as a function of the electron energy. Solid blue lines represent the trajectories starting at the essential saddle points which appear at the maximum of the electric field whereas the dashed red lines are for the essential saddle points which appear at the minimum of the electric field. The laser field parameters are $\omega_{\mathrm{L}} = 1.55\mathrm{eV}$, $I = 3.125 \times 10^{13}\mathrm{W/cm}^2$ and $N_{\mathrm{rep}} = 3$.

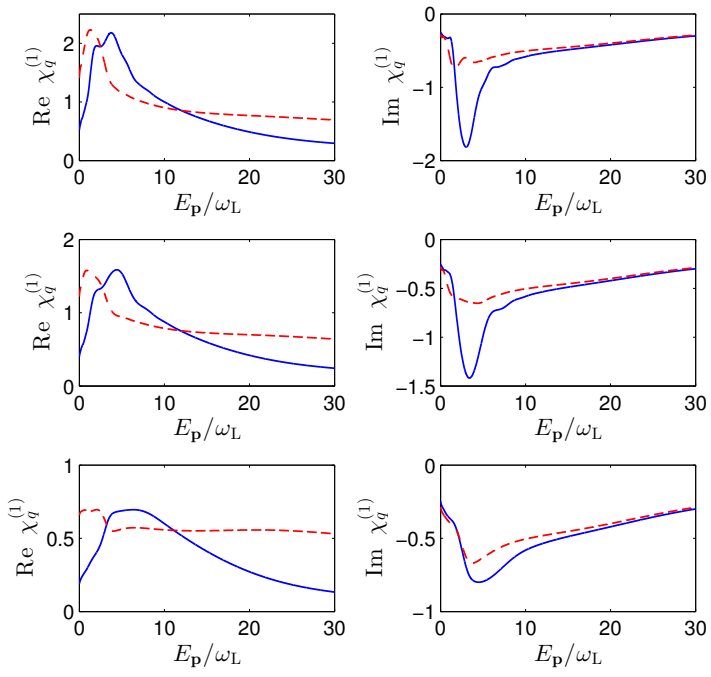

Figure 4. The same as in Fig. 3 but for the generalized eikonal, $\chi_q^{(1)}(\boldsymbol{p},\phi_s)$, given by Eq. (38).

being that the generalized eikonal, $\chi_q^{(1)}(\boldsymbol{p}, \phi_s)$, defined by Eq. (38), is not singular even for those trajectories which come back to the potential center (see, Fig. 4). Thus, the lack of spurious behavior of trajectories returning back to the vicinity of the parent ion makes the approach presented here an attractive tool for investigations of ionization, rescattering and high-order harmonic generation by strong laser pulses. This includes also more complex systems such as diatomic molecules or fullerenes.

5. Conclusions

In this paper, we have presented the basics of the eikonal perturbation theory. We have focused on its first term, the generalized eikonal approximation [27], when applied to strong-field ionization. A comparison with the original eikonal approximation, introduced in Refs. [20, 21], was performed. It turned out that, while the original eikonal is singular for electron trajectories which return to the Coulomb potential center, the generalized eikonal does not share this property. Thus, in contrast to the original eikonal, the newly developed approach does not lead to unphysical behavior of the probability distributions of ionization [27]. Its further applications to rescattering and high-order harmonic generation are being considered.

Acknowledgments

This work was supported by the Polish National Science Center (NCN) under Grant No. 2012/05/B/ST2/02547. Moreover, F.C.V. acknowledges the support from the Foundation for Polish Science International PhD Projects Programme co-financed by the EU European Regional Development Fund.

References

[1] Keldysh L V 1965 *Sov. Phys. JETP* **20** 1307
[2] Faisal F H M 1973 *J. Phys. B* **6** L89
[3] Reiss H R 1980 *Phys. Rev. A* **22** 1786
[4] Becker W, Lohr A and Kleber M 1994 *J. Phys. B* **27** L325
[5] Lewenstein M, Kulander K C, Schafer K J and Bucksbaum P H 1995 *Phys. Rev. A* **51** 1495
[6] Milošević D B 2013 *Phys. Rev. A* **88** 023417
[7] Jain M and Tzoar N 1978 *Phys. Rev. A* **18** 538
[8] Cavaliere P, Ferrante G and Leone C 1980 *J. Phys. B* **13** 4495
[9] Kamiński J Z 1986 *Phys. Scr.* **34** 770
[10] Kamiński J Z 1988 *Phys. Rev. A* **37** 622
[11] Popov V S 2004 *Phys. Usp.* **47** 855
[12] Popov V S 2005 *Phys. At. Nucl.* **68** 686
[13] Gribakin G F and Kuchiev M Yu 1997 *Phys. Rev. A* **55** 3760
[14] Popruzhenko S V, Paulus G G and Bauer D 2008 *Phys. Rev. A* **77** 053409
[15] Popruzhenko S V 2014 *J. Phys. B* **47** 204001
[16] Saha B C, Sarkar K and Ghosh A S 1973 *J. Phys. B* **6** 2303
[17] Byron Jr. F W and Joachain Ch J 1977 *Phys. Rev. A* **15** 128
[18] Joachain Ch J 1975 *Quantum Collision Theory* (Amsterdam: North Holland)
[19] Kamiński J Z 1984 *Acta Phys. Pol. A* **66** 517
[20] Molière G 1947 *Z. Naturforsch.* **2** 133
[21] Glauber R J 1959 *Lectures in Theoretical Physics* ed. W E Brittin and L G Dunham (New York: Interscience) vol 1 pp 315-414
[22] Banerji J and Mittelman M H 1981 *J. Phys. B* **14** 3717
[23] Krstić P and Mittleman M H 1982 *Phys. Rev. A* **25** 1568
[24] Reiss H R and Krainov V P 1996 *Proc. SPIE* **39** 2796
[25] Krainov V P 1997 *J. Opt. Soc. Am. B* **14** 425
[26] Smirnova O, Spanner M and Ivanov M 2008 *Phys. Rev. A* **77** 033407
[27] Cajiao Vélez F, Krajewska K and Kamiński J Z 2015 *Phys. Rev. A* **91** 053417